Journal Name

Dynamic Article Links ►

Cite this: DOI: 10.1039/c0xx00000x

www.rsc.org/xxxxxx

ARTICLE TYPE

Surface Modification of TiO_2 with Metal Oxide Nanoclusters: a Route to Composite Photocatalytic Materials

Michael Nolan*[a]

Received (in XXX, XXX) Xth XXXXXXXXX 20XX, Accepted Xth XXXXXXXXX 20XX

DOI: 10.1039/b000000x

Density functional theory simulations show that modifying rutile TiO_2 with metal oxide nanoclusters produces composite materials with potential visible light photocatalytic activity.

Developing visible light active photocatalysts for hydrogen production is a major activity. TiO_2 has desirable qualities of being cheap, readily available, stable and non-toxic, but pure TiO_2 is not suitable, since it primarily absorbs in the ultra violet. Modifying TiO_2 to allow visible light absorption is well studied, reviewed in refs. 1 and 2.

Many efforts in enabling visible light absorption have focused on substitutional cation or anion doping at the Ti or O sites[3-11], or cation-anion co-doping[12-14]. However, there are issues with substitutional doping of TiO_2, such as dopant incorporation /solubility, stability and charge recombination. Strategies for surface modification of TiO_2 shifting the band gap to the visible while improving photocatalytic efficiency are being researched.

The dye sensitised solar cell (DSSC), developed by Gratzel and co-workers[15,16] is a paradigm in this regard, in which a dye molecule is adsorbed at the surface of TiO_2 nanoparticles and plays the role of a visible light absorber. Metal sulphide quantum dots adsorbed on TiO_2 have been studied[17]. Recent developments have shown that oxide-oxide heterostructures[18-23] can display visible light absorption and improved photocatalytic activity over the pure oxides. Examples include $Bi_3Ti_4O_{12}$-TiO_2[18], $BiVO_4$-WO_3[19] and BiOBr-$ZrFe_2O_4$[20]. The valence and conduction band alignments of the oxides in the heterostructure are postulated to allow visible light absorption and charge separation[18-23].

One can conceive of using metal oxide nanoclusters adsorbed at a TiO_2 surface as a composite photocatalytic material, with the oxide nanocluster playing a role similar to the dye in a DSCC or the sulphide quantum dot. A visible light active heterostructure of iron oxide supported on TiO_2 has been reported[21-23], in which *dispersed, molecular sized FeO_x species* are supported on TiO_2. Atomic layer deposition[21] and a chemisorption-calcination cycle[22,23] have been used to fabricate the heterostructure, which demonstrates band gap narrowing and visible light absorption, as well as reduced charge recombination, as characterised by photoluminescence spectroscopy[21-23]. Band gap narrowing is suggested to arise from the presence of iron oxide states in the band gap, shifting the valence band edge upwards. The heterostructure approach has advantages over substitutional doping; alleviating many issues and allows fine tuning of properties through composition.

We have used first principles density functional theory (DFT), with Hubbard correction for on-site Coulomb interactions (DFT+U) to study TiO_2 nanoclusters supported on TiO_2 and we find that the heterostructures have reduced band gaps, and will facilitate electron-hole separation[24]. To investigate other heterostructures composed of metal oxide nanoclusters supported on TiO_2, this paper presents DFT+U studies of metal oxide nanoclusters adsorbed on the rutile (110) surface. The rutile TiO_2 (110) surface is chosen as rutile is the most stable TiO_2 phase, and the (110) surface, as well as being well studied [25-28], is energetically the most stable surface among the low index surfaces. Rutile (110) is a suitable substrate for deposition of other species[29,30].

In the calculations, for which the computational details are presented in the ESI (sec. S1), we adsorb and relax the metal oxide nanoclusters on the rutile (110) surface. The oxide nanoclusters are Sn_2O_4, Cr_2O_4/Cr_2O_3, Mo_2O_4 and Zr_2O_4. This size of nanocluster is studied since refs. 22 and 23 indicate that the FeO_x species supported on TiO_2 are of this size. The supported oxide nanoclusters are in a size regime realisable experimentally. The minimum energy structures for free M_2O_4 and M_2O_3 clusters are shown in figure 1(f) (see ESI) and are consistent with the global minima for these stoichiometries[31,32]. Two oxidation states are considered for CrO_x since the energy required for the transformation of $Cr_2O_4 \leftrightarrow Cr_2O_3$ is small, see ESI, sec. S2.

The relaxed adsorption structures for the clusters supported on TiO_2 are shown in figure 1. The adsorption energies, computed relative to a bare (110) rutile surface and a free oxide nanocluster lie in the range of -3.43 eV (Cr_2O_4) to -7 eV (Zr_2O_4), indicating strong binding between the oxide cluster and the TiO_2 surface.

For all supported oxides, the cations of the cluster bind to bridging and in-plane oxygen atoms of TiO_2. Sn_2O_4, Zr_2O_4 and Cr_2O_3 adsorb at the TiO_2 surface using three cluster oxygen atoms to bond to surface 5-fold coordinated Ti. In Cr_2O_4 and Mo_2O_4, two cluster oxygen atoms bind with 5fold coordinated surface Ti. In the Sn_2O_4 and Zr_2O_4 clusters, the fourth oxygen bridges the cluster cations, while in Cr_2O_4 and Mo_2O_4, two oxygen atoms of the cluster do not interact with surface Ti.

In examining the geometry of the cluster at the surface, we see multiple new metal-O bonds between the cluster and the surface, which make the cations in the cluster 6 coordinate, which is a favourable coordination environment. Compared to the gas phase clusters, adsorption tends to break the symmetry of the cluster. Metal-oxygen distances in the adsorbed cluster are lengthened

compare to the free oxide clusters. The distances for the cluster cation to surface oxygen are longer than in the corresponding oxide of the cation, but are nonetheless consistent with formation of a bond between the cation and surface oxygen. Finally, Ti-O distances to oxygen of the supported cluster are generally typical of TiO_2. We note that supported Cr_2O_4 has the least cluster-surface bonds (see complete geometry data in sec. S3, ESI) and the smallest adsorption energy, while Zr_2O_4 has the most cluster-surface bonds and this is consistent with the corresponding adsorption energies, so that maximising the number of new cluster-surface bonds enhances adsorption of the oxide cluster[24].

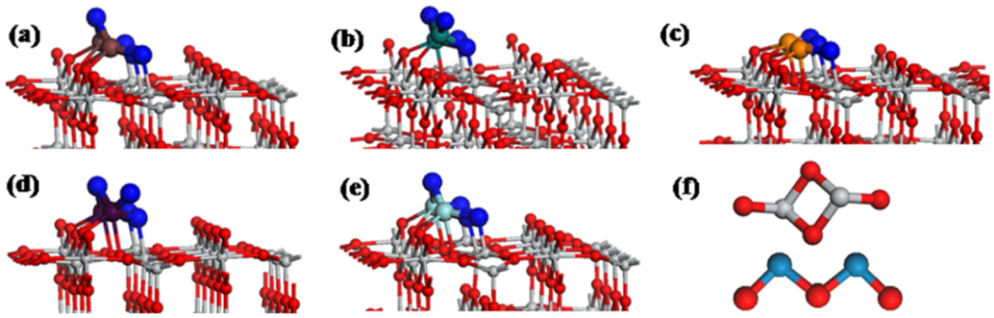

Fig. 1 Relaxed atomic structure of metal oxide clusters supported on the rutile TiO_2 (110) surface. (a) Sn_2O_4, (b) Cr_2O_4, (c) Cr_2O_3 (d) Mo_2O_4 and (e) Zr_2O_4. Part (f) shows the most stable structure for an M_2O_4 and an M_2O_3 nanocluster. In (a)-(e), Ti of the surface is grey, O from the surface is red, O from the cluster is large blue spheres and the cations in the clusters are coloured differently for each element. In (f) the cluster oxygen are red.

The alignments of the electronic states of the two oxides determine the photocatalytic properties. In experiments, the absorption spectra display a shift to longer wavelength, indicative of band gap narrowing. Photoluminescence spectra can be used to study charge recombination. XPS has been used to determine cation oxidation states. From these analyses the relative positions of the valence and conduction bands have been discussed.

In the present calculations, we examine the electronic density of states (EDOS), projected onto cation and oxygen states from the support and the cluster (PEDOS) to determine the impact of surface modification on the electronic structure of the composite; the PEDOS of the bare rutile (110) surface is shown in the ESI (sec. S4). Bader charge analysis[33] allows identification of cation oxidation states. Formation of an interface between the support and the cluster allows the alignments of the surface and cluster electronic states to be determined. It is this alignment of the electronic states upon modification of TiO_2 by the cluster that is of interest; ref. 20 highlights the importance of the interface in the heterostructure.

Figure 2 shows the PEDOS for Sn 5*s,* Zr 5*d* states and oxygen 2*p* states from the surface and the cluster for the composites. Analysing the electronic structure shows that the Zr_2O_4-TiO_2 composite shows no change in the band gap from pure TiO_2. The ZrO_2 derived electronic states lie below the VB and above the CB of TiO_2; this arises from the very large band gap of ZrO_2 structures. Analysis of a Hf_2O_4-TiO_2 heterostructure gives the same conclusion – oxides with band gaps much larger than of that of TiO_2 will not be suitable for reducing the band gap of TiO_2; see sec. S5 in the ESI.

The top of the valence band of Sn_2O_4-modified TiO_2 is derived from the TiO_2 surface, while the bottom of the conduction band is derived from empty Sn 5*s* states of the cluster, shifting the conduction band down in energy by 0.2 eV, and narrowing the band gap. Although band gap changes determined with DFT+U (for which the band gap remains underestimated) will be qualitative, the shifts in the valence or conduction band edges should be useful for comparing trends across a series of materials.

The band gap reduction with Sn_2O_4 modified TiO_2 is small and may not be sufficient to shift absorption to the visible.

For supported Cr_2O_4 and Mo_2O_4 nanoclusters (see ESI, sec. S6 for Cr_2O_3), the PEDOS are shown in figure 3. In this case, the top of the valence band is pushed upwards, by between 0.4 eV and 0.6 eV, due to the presence of electronic states from the adsorbed cluster. This shift is large enough to narrow the band gap into the visible, so that if the TiO_2 surface can be modified by adsorption of these metal oxides, visible light absorption will take place.

Bader charges have been computed for the cations in the adsorbed cluster and in the surface (see ESI, table S2). For Ti, the Bader charges take values typical of Ti^{4+}, while the various cluster cations also take Bader charges consistent with their expected oxidation states. Thus, there is no charge transfer between the supported cluster and the TiO_2 surface.

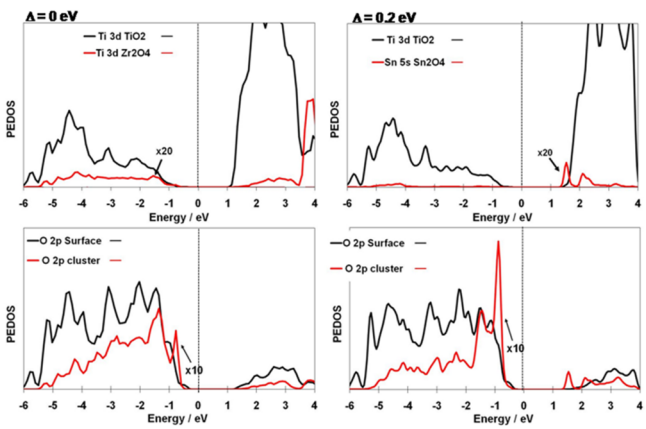

Fig. 2 PEDOS projected onto Ti 3*d*, Sn 5*s*, Zn 5*d* and O 2*p* states for Sn_2O_4 and Zr_2O_4 supported on the rutile (110) surface. **Left panel:** Sn_2O_4, **Right panel:** Zr_2O_4. The shift in the valence-conduction band energy gap is given at the top of each panel in eV. The Fermi level is indicated by the vertical line at 0 eV. The cluster PEDOS are enhanced by the factors given in the figure, since there are 2 cations and 4 anions, compared with 96 surface cations and 192 cluster anions.

The alignments of the surface and cluster electronic states in CrO_x and Mo_2O_4-modified TiO_2 have the consequence that upon excitation of an electron by visible light from the nanocluster states to the CB, the excited electron will migrate to the TiO_2 surface, while the resulting hole will be found on the cluster. Even if the cluster has a short charge diffusion length, the dimensions of the cluster mitigate against this, as discussed for iron oxide modified TiO_2[20-23]. For Sn_2O_4, excitation of electrons will result in holes migrating to the TiO_2 surface and electrons to the cluster, specifically in the Sn 5*s* states, which are good conducting states. Thus, the heterostructure approach facilitates separation of electrons and holes after excitation, which is necessary to reduce charge recombination and is the second factor in enabling improved photocatalytic activity. The modifications of TiO_2 with metal oxide clusters thus shares some similarities with other approaches to surface modified TiO_2 for visible light activity, but provides another route to tune properties.

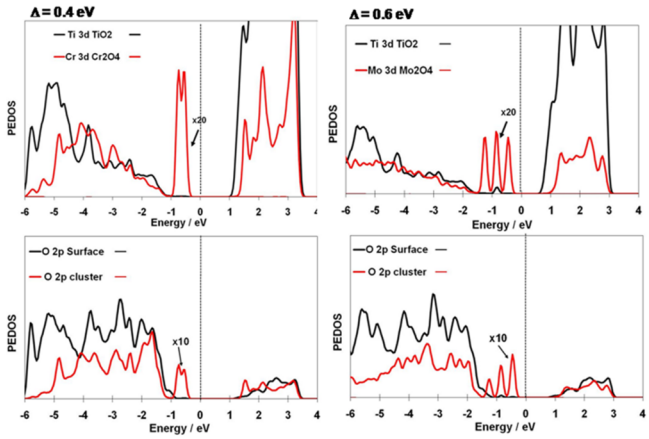

Fig. 3 PEDOS projected onto Ti 3*d*, Cr 3*d*, Mo 4*d* and O 2*p* states for Sn_2O_4 and Zr_2O_4 supported on the rutile (110) surface. **Left panel:** Cr_2O_4, **Right panel:** Mo_2O_4. The shift in the valence-conduction band energy gap is given at the top of each panel in eV. The Fermi level is indicated by the vertical line at 0 eV. The cluster PEDOS are enhanced by the factors given in the figure, since there are 2 cations and 4 anions, compared with 96 surface cations and 192 cluster anions.

In conclusion, we have shown that TiO_2 modified with metal oxide nanoclusters, in particular CrO_x and Mo_2O_4, is a heterostructured material system with the necessary properties to be a visible light active photocatalytic material. With advances in synthesis of heterostructured composites, this is another approach to developing visible light active photocatalytic materials.

Support from Science Foundation Ireland through a Starting Investigator Research Grant, ("EMOIN": SFI 09/SIRG/I1620) is acknowledged, as are computing resources funded by SFI and provided by the SFI/Higher Education Authority Funded Irish Centre for High End Computing.

Notes and references

[a] *Tyndall National Institute, University College Cork, Lee Maltings, Prospect Row, Cork, Ireland. Email: michael.nolan@tyndall.ie*

† Electronic Supplementary Information (ESI) available: details of the computational methods employed, geometry data, TiO_2 (110) surface EDOS, data on CrO_x and Hf_2O_4 supported on TiO_2. See DOI: 10.1039//

1 A. Fujishima, X. Zhang and D. A. Tryk, *Surf. Sci. Rep.* 2008, **63**, 515.
2 X. L. Nie, S. P. Zhou, G. Maeng and K. Sohlberg, *Int. J. Photoenergy* 2009**,** 294042
3 Y. Cui, H. Du and L. S. Wen, *J. Mat. Sci. and Tech.*2008**, 24**, 675
4 H. W. Peng, J. B. Li, S. S. Li and J. B. Xia, *J. Phys. Cond. Matt.* 2008, **20**, 125207
5 C. Di Valentin, G. Pacchioni, H. Onishi and A. Kudo, *Chem. Phys. Lett.* 2009, **469**, 166
6 J. G. Yu, Q. J. Xiang and M. H. Zhou, *Appl. Cat. B Environmental* 2009, **90**, 595
7 L. Bian, M. X. Song, T. L. Zhou, X. Y. Zhao and Q. Q. Dai, *J. Rare Earths* 2009, **27**, 461
8 C. Di Valentin, E. Finazzi, G. Pacchioni, A. Selloni, S. Livraghi, M. C. Paganini and E. Giamello, *Chem. Phys*. 2007**, 339**, 44
9 A. M. Czoska, S. Livraghi, M. Chiesa, E. Giamello, S. Agnoli, G. Granozzi, E. Finazzi, C. Di Valentin and G. Pacchioni, *J. Phys. Chem C* 2008, **112**, 8951
10 R. Long and N. J. English, *J. Phys. Chem. C* 2010, **114**, 11984
11 J. W. Zheng, A. Bhattcahrayya,P. Wu, Z. Chen, J. Highfield, Z. L. Dong and R. Xu, *J. Phys. Chem. C* 2010, **114**, 7063
12 Y. Q. Gai, J. B. Li, S. S. Li, J. B. Xia and S. H. Wei, *Phys. Rev. Lett.* 2009, **102**, 036402
13 W. G. Zhu, X. F. Qiu, V. Iancu X. Q. Chen, H. Pan, W. Wang, N. M. Dimitrijevic, T. Rajh,H. M. Meyer, M. P. Paranthaman, G. M. Stocks, H. H. Weitering, B. H. Gu, G. Eres and Z. Y. Zhang, *Phys. Rev. Lett.* 2009, **103**, 2264101
14 J. Zhang, C. X. Pan, P. F. Fang, J. H. Wie and R. Xiong, *ACS Applied Materials and Interfaces* 2010, **2,** 1173
15 M. Gratzel, *MRS Bull.,* 2005, **30,** 23
16 D. Wei, *Int. J. Mol. Sci.,* 2010, **11,** 1103
17 G. Ai, W. Sun, X. Gao, Y. Zhang, and L-M. Peng, *J. Mat. Chem.* 2011, **21,** 8749
18 T. Cao, Y. Li, C. Wang, Z. Zhang, M. Zhang, C. Shao and Y. Liu, *J. Mat. Chem.* 2011, **21,** 6922
19 S. J. Hong, S. Lee, J. S. Jang and J. S. Lee, *Energy Envir. Science,* 2011, **4,** 1781
20 L. Kong, Z. Jiang, T. Xiao, L. Lu, M. O. Jones and P. P. Edwards, *Chem. Comm.,* 2011, **47, 5512**
21 J. A. Libera, J. W. Elam, N. F. Sather, T. Rajh and N. M. Dimitrijevic, *Chem. Mat.*, 2010, **22**, 409
22 H. Tada, Q. Jin, H. Nishijima, H. Yamamoto, M. Fujishima, S-i. Okuoka, T. Hattori, Y. Sumida and H. Kobayashi, *Angew Chem.* 2011, **50,** 3501
23 Q. Jin, N. Fujishima and H. Tada, *J. Phys. Chem. C* 2011, **115,** 6478
24 A. Iwaszuk and M. Nolan, *Phys. Chem. Chem. Phys.* 2011, **13**, 4963
25 U. Diebold, *Surf. Sci. Rep.* 2003, **48,** 53
26 Z. Dohnalek, I. Lyubinetsky and R. Rousseau, *Prog. In Surf. Sci.,* 2010, **85**, 161
27 E. Wahlstrom, E. K. Vestergaard, R. Schaub, A. Ronnau, M. Vestergaard, E. Laegsgaard, I. Stensgaard and F. Besenbacher, *Science* 2004, **303**, 511
28 R. Schaub, E. Wahlstrom, A. Ronnau, E. Laegsgaard, I. Stensgaard and F. Besenbacher, *Science* 2003, **299**, 377
29 C. L. Pang, R. Lindsay and G. Thornton , *Chem. Soc. Rev.,* 2008, **37**, 2328
30 G. D. Sheng, J. X. Li, S. W. Wang and X. K. Wang, *Prog. In Chem.,* 2009, **21**, 2492
31 S. A. Shevlin and S. M. Woodley, *J. Phys. Chem. C* 2010, **114,** 17333
32 A. Walsh and S. M. Woodley, *Phys. Chem. Chem. Phys.,* 2010, **12,** 8446
33 G. Henkelman, A. Arnaldsson and H. Jónsson, *Comput. Mater. Sci.*, 2006, **36**, 254